# Pregnane X receptor knockout mice display osteopenia with reduced bone formation and enhanced bone resorption

**Kotaro Azuma[1], Stephanie C Casey[2], Masako Ito[3], Tomohiko Urano[1,4], Kuniko Horie[5], Yasuyoshi Ouchi[1], Séverine Kirchner[2], Bruce Blumberg[2]** and **Satoshi Inoue[1,4,5]**

[1]Department of Geriatric Medicine, Graduate School of Medicine, The University of Tokyo, 7-3-1 Hongo, Bunkyo-ku, Tokyo 113-8655, Japan

[2]Department of Developmental and Cell Biology, University of California, Irvine, California 92697-2300, USA

[3]Division of Radiology, Nagasaki University Hospital, 1-12-4 Sakamoto, Nagasaki 852-8523, Japan

[4]Department of Anti-Aging Medicine, Graduate School of Medicine, The University of Tokyo, 7-3-1 Hongo, Bunkyo-ku, Tokyo 113-8655, Japan

[5]Division of Gene Regulation and Signal Transduction, Research Center for Genomic Medicine, Saitama Medical University, 1397-1 Yamane, Hidaka, Saitama 350-1241, Japan

(Correspondence should be addressed to S Inoue at Department of Geriatric Medicine, Graduate School of Medicine, The University of Tokyo; Email: inoue-ger@h.u-tokyo.ac.jp)

## Abstract

The steroid and xenobiotic receptor (SXR) and its murine ortholog pregnane X receptor (PXR) are nuclear receptors that are expressed mainly in the liver and intestine where they function as xenobiotic sensors. In addition to its role as a xenobiotic sensor, previous studies in our laboratories and elsewhere have identified a role for SXR/PXR as a mediator of bone homeostasis. Here, we report that systemic deletion of PXR results in marked osteopenia with mechanical fragility in female mice as young as 4 months old. Bone mineral density (BMD) of PXR knockout (PXRKO) mice was significantly decreased compared with the BMD of wild-type (WT) mice. Micro-computed tomography analysis of femoral trabecular bones revealed that the three-dimensional bone volume fraction of PXRKO mice was markedly reduced compared with that of WT mice. Histomorphometrical analysis of the trabecular bones in the proximal tibia showed a remarkable reduction in bone mass in PXRKO mice. As for bone turnover of the trabecular bones, bone formation is reduced, whereas bone resorption is enhanced in PXRKO mice. Histomorphometrical analysis of femoral cortical bones revealed a larger cortical area in WT mice than that in PXRKO mice. WT mice had a thicker cortical width than PXRKO mice. Three-point bending test revealed that these morphological phenotypes actually caused mechanical fragility. Lastly, serum levels of phosphate, calcium, and alkaline phosphatase were unchanged in PXRKO mice compared with WT. Consistent with our previous results, we conclude that SXR/PXR promotes bone formation and suppresses bone resorption thus cementing a role for SXR/PXR as a key regulator of bone homeostasis.

*Journal of Endocrinology* (2010) **207,** 257–263

## Introduction

The steroid and xenobiotic receptor (SXR) and its murine ortholog pregnane X receptor (PXR) (also known as PAR and NR1I2) are nuclear receptors that are activated by various endogenous and dietary substances, pharmaceutical agents, and xenobiotic compounds (Zhou *et al.* 2009). SXR/PXR is mainly expressed in the liver and intestine (Blumberg *et al.* 1998), where it functions as a xenobiotic sensor by inducing the genes involving detoxification and drug excretion (Blumberg *et al.* 1998, Synold *et al.* 2001). The expression of SXR/PXR was also detected at lower levels in the kidney, lung (Miki *et al.* 2005), bone (especially in osteoblasts; Tabb *et al.* 2003), and peripheral mononuclear cells (Albermann *et al.* 2005). However, the functions of SXR/PXR in these cells remain largely unclear.

Recently, we have found that vitamin K also functions as a ligand for SXR/PXR and demonstrated SXR/PXR-dependent biological functions of vitamin K in the bone (Tabb *et al.* 2003) and in hepatocellular carcinoma cells (Azuma *et al.* 2009). Vitamin K has been shown to have an effect on bone fracture prevention (Shiraki *et al.* 2000, Cockayne *et al.* 2006) and is clinically used for the treatment of osteoporosis in Japan, Korea, and Thailand. Until recently, vitamin K was primarily known as a co-enzyme for γ-carboxylase. Some bone-specific proteins such as osteocalcin (Price *et al.* 1976) and matrix Gla protein (Luo *et al.* 1997) require γ-carboxylation. We demonstrated γ-carboxylation-independent and SXR/PXR-dependent vitamin K function in the bone by showing abolished bone marker induction in PXR-deficient osteoblasts (Tabb *et al.* 2003). Furthermore, several SXR/PXR target genes


DOI: 10.1677/JOE-10-0208
0022–0795/10/0207–257 
Online version via http://www.endocrinology-journals.org

expressed in bone such as *tsukushi*, *matrilin-2*, *CD14*, and *Msx2* have been identified by our group and other groups (Ichikawa *et al.* 2006, Igarashi *et al.* 2007).

SXR/PXR has also been shown to affect the vitamin D receptor (VDR) function by inducing the enzyme CYP3A4 in the liver and intestine, which catabolizes vitamin D among its many substrates (Zhou *et al.* 2006*a*). Considering the roles of vitamin D on calcium and phosphate homeostasis, SXR/PXR could affect bone metabolism through the cross talk with VDR. More recently, induction of the phosphate transporter, SLC34A2, in the intestine by SXR/PXR was reported (Konno *et al.* 2010). This group showed that PXR knockout (PXRKO) mice are hypophosphatemic and consequently experience bone loss. Taken together, these reports indicate that SXR/PXR expression outside the bone tissue could affect bone metabolism indirectly through the regulation of calcium and phosphate homeostasis.

In this study, we characterized the histomorphometrical phenotype of PXRKO mice to understand the roles of SXR/PXR in the bone tissue more precisely. Our results demonstrated that loss of SXR/PXR enhanced bone resorption and reduced bone formation in the trabecular bones and decreased thickness in the cortical bones. Moreover, these mice had normal levels of serum phosphate and calcium, suggesting that SXR/PXR regulates other bone-specific processes, which are deficient and lead to bone loss in PXRKO mice. Thus, SXR/PXR plays a key role in bone homeostasis.

## Materials and Methods

### *Animal experiments*

The generation of the PXRKO mice has previously been described (Xie *et al.* 2000). The PXRKO mice were maintained in the 129/Sv background. The animals were housed in a temperature-controlled room (22 °C) with a 12 h light:12 h darkness schedule. Animals had free access to water and were fed a standard laboratory chow. Age-matched 129/Sv wild-type (WT) mice were used as controls and maintained under the same conditions. Female mice of age 4 months were injected with 20 mg/kg tetracycline hydrochloride s.c. 5 days before killing, followed by 20 mg/kg calcein s.c. injection 3 days later. Mice were killed 30 h after calcein injection, and both the legs were dissected. The left legs were preserved with 70% ethanol for histomorphometrical analysis, while the right legs were fixed with 4% paraformaldehyde in 0·1 M phosphate buffer for bone mineral density (BMD) measurement and micro-computed tomography (micro-CT) analysis. The U.C. Irvine Institutional Animal Care and Use Committee approved all animal procedures.

### *BMD measurements*

The BMD of the right femoral bones was measured by dual-energy X-ray absorptiometry using the Lunar PIXImus2 densitometer (GE Medical Systems, Madison, WI, USA). The whole right leg fixed with 4% paraformaldehyde in 0·1 M phosphate buffer was placed in a specimen tray. After calibration, duplicate cycles of four scans were obtained. The region of the femoral bone was selected and analyzed.

### *Quantitative micro-computed tomography*

Quantitative micro-CT scanning of the femoral trabecular bone of the distal metaphysis of PXRKO mice and WT mice was performed. The femoral trabecular bones of the distal metaphysis were analyzed by the micro-CT system (μCT-40; Scanco Medical, Bassersdorf, Switzerland), as reported previously (Rüegsegger *et al.* 1996). Using two-dimensional data from scanned slices, three-dimensional analysis was performed to calculate morphometrical indices including bone volume density (bone volume (BV)/tissue volume (TV)), trabecular thickness (Tb.Th.)=2×BV/bone surface (BS), trabecular number (Tb.N.)=(BV/TV)/Tb.Th., trabecular separation (Tb.Sp.)=(1/Tb.N.)−Tb.Th., connectivity density representing the maximum number of branches broken to divide the structure in two parts, and the structure model index (SMI), an indicator of plate-like trabecular architecture (score 0) versus rod-like trabecular architecture (score 3).

### *Bone histomorphometry*

Mice were injected with 20 mg/kg tetracycline hydrochloride s.c. 5 days before killing. Then, they were injected with 20 mg/kg calcein s.c. 3 days later. Mice were killed 30 h after calcein injection, and the left legs were dissected for bone histomorphometrical analysis. The legs were fixed with 70% ethanol, and soft tissues were removed. Bone histomorphometry was performed on undecalcified sections with the Villanueva Bone Stain (Villanueva & Lundin 1989). The region of trabecular bone 100–700 μm distal to the lower margin of the growth plate in the proximal tibia was selected for the measurement of trabecular bones. The parameters measured for the trabecular bone included the total TV, BV, BS, eroded surface (ES), osteoclast surface (Oc.S), number of osteoclasts (N.Oc), osteoid volume (OV), mineralizing surface (MS), and osteoblast surface (Ob.S). As for N.Oc, number of mononuclear osteoclast (N.Mo.Oc.) and number of multinuclear osteoclasts (N.Mu.Oc.) were counted separately. Under fluorescence microscope, single- and double-labeled surfaces (sLS and dLS respectively), labeled thickness (L.Th.) were measured. The secondary parameters calculated based on these measurements included BV/TV, Oc.S/BS, N.Oc/BS, OV/BV, MS/BS, Ob.S/BS, mineral apposition rate (MAR)=L.Th./days of labeling interval, and bone formation rate (BFR)=((sLS/2+dLS)×MAR×365). For the measurement of cortical bone, horizontal section of the diaphysis at the center of the femoral bone was used. The parameters measured for the cortical bone included cortical bone area and cortical width. Under fluorescence microscope, ES and MS were observed.

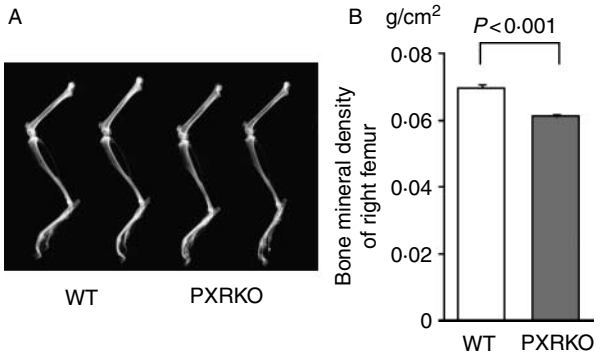


**Figure 1** Osteopenia in PXR knockout mice. (A) Two representative radiographs of left legs of wild-type (WT) mice and PXR knockout (PXRKO) mice are shown. No apparent gross abnormality was observed in PXRKO mice. (B) Bone mineral densities of right femurs of WT ($n=8$) and PXRKO ($n=8$) mice are shown.

*Serum analysis*

Blood was collected from WT and KO animals via direct cardiac puncture immediately postmortem. Blood was allowed to coagulate at room temperature for 90 min and centrifuged at 4000 ***g*** for 15 min, and serum was carefully removed and stored at 4 °C until use. Serum levels of calcium and inorganic phosphate were measured by UCI Pathology Services using arsenazo IV (calcium) or phosphomolybdate (phosphate).

*Biomechanical analysis of femoral bones*

The mechanical properties of the diaphysis of femoral bones were evaluated by three-point bending test. Load was applied midway between two supports placed 8 mm apart. The femur was positioned so that the loading point was at the center of the femoral diaphysis, and bending occurred in the medial–lateral axis. The bending test was done in a saline bath at 37 °C. Load–displacement curves were recorded at a cross-head speed of 5 mm/min using a material testing machine MZ500S (Maruto, Co., Ltd, Tokyo, Japan). The maximum load and stiffness were analyzed using software CTRwin (System Supply Co., Ltd, Kanagawa, Japan).

*Statistical analysis*

Data are expressed as the mean+S.E.M. Differences between the mean values were analyzed using the unpaired Student's *t*-test.

## Results

*Decreased BMD in PXRKO mice*

To examine the effects of PXR on the bone tissue, we utilized PXRKO mice. PXRKO mice were viable, fertile, bred with normal Mendelian distribution, and did not exhibit any overt phenotypic change as described previously (Staudinger *et al.* 2001). We first evaluated the gross appearance of entire leg of 4-month-old female PXRKO mice using radiographical images. No apparent gross abnormality in shape was observed in the leg bones of female PXRKO mice compared with that of female WT mice, although the radiographs suggest a slight decrease in bone density in the femoral bones of PXRKO mice (Fig. 1A). The BMD of femoral bone was quantified by dual-energy X-ray absorptiometry (DXA). Notably, the BMD of PXRKO mice was significantly

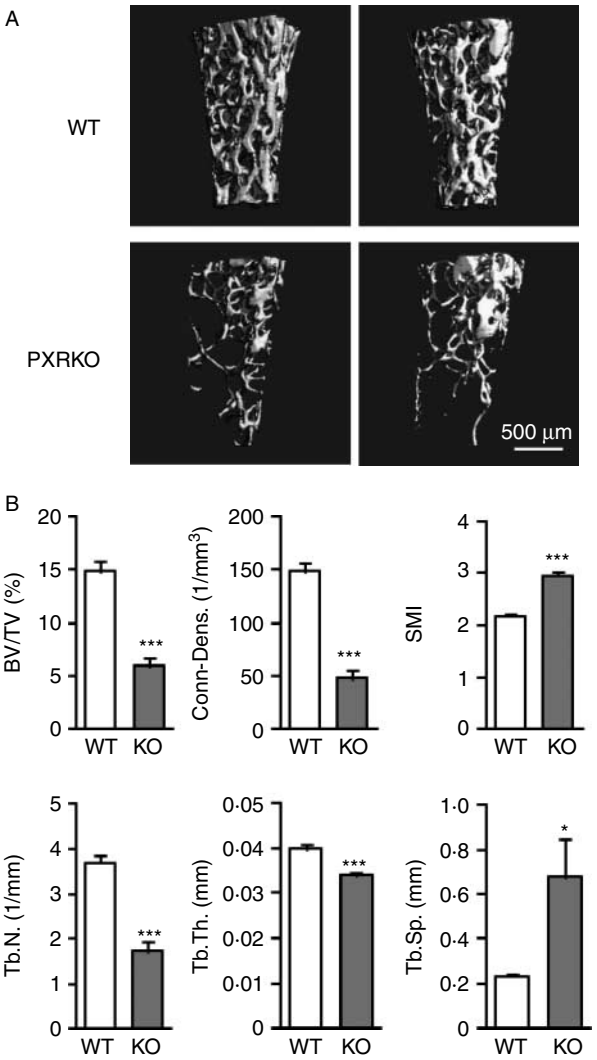


**Figure 2** Three-dimensional change in the trabecular bones of PXR knockout mice. (A) Representative three-dimensional micro-CT images of the femoral trabecular bones are shown. Upper panels: wild-type (WT) mice. Lower panels: PXR knockout mice (PXRKO). (B) Microstructural parameters (BV/TV, three-dimensional bone volume fraction per tissue volume; Conn-Dens., connectivity density; SMI, structure model index; Tb.N., trabecular number; Tb.Th., trabecular thickness; Tb.Sp., trabecular separation) of femoral trabecular bones of wild-type (WT; $n=8$) and PXR knockout (KO; $n=8$) mice derived from micro-CT analysis are shown. ***$P<0·001$; *$P<0·05$.

decreased compared with the BMD of WT mice (WT: 0·0679±0·0014 g/cm$^2$, PXRKO: 0·0588±0·0011 g/cm$^2$, $P<0·001$; Fig. 1B). To exclude the possibility that difference of body weights between PXRKO mice and WT mice influenced decreased BMD in PXRKO mice, growth of PXRKO mice was compared with that of WT mice. The mean body weight of PXRKO mice at 1 month of age ($n=3$) was 14·16±0·72 g, while the mean body weight of WT mice at the same month of age ($n=8$) was 15·07±0·38 g ($P=0·26$). The mean body weight of PXRKO mice at 2 months of age ($n=3$) was 19·68±0·66 g, while the mean body weight of WT mice at the same month of age ($n=10$) was 18·84±0·45 g ($P=0·37$). Finally, the mean body weight of PXRKO mice at 4 months of age ($n=6$) was 22·38±0·51 g, while the mean body weight of WT mice at the same month of age ($n=3$) was 20·71±0·60 g ($P=0·09$). Therefore, there was no significant difference in growth between PXRKO mice and WT mice at least up to 4 months of age when we analyzed the bone phenotype.

### *Microstructural differences in trabecular bones of PXRKO mice*

Next, three-dimensional bone microstructure was evaluated using micro-CT analysis. These studies revealed a remarkable bone loss in femoral trabecular bones of 4-month-old female PXRKO mice (Fig. 2A). Calculation of standard three-dimensional parameters of the trabecular bones revealed a significant and substantial decrease in BV/TV of PXRKO mice compared with that of WT mice (WT: 14·85±1·01%, PXRKO: 5·92±0·79%, $P<0·001$). This decrease was associated with changes in bone microstructure, such as reduced trabecular connectivity, thickness and number, accompanied by increased Tb.Sp. The SMI was also increased in PXRKO mice, indicating transformation of the shape from plate-like structure to fragile rod-like structure (Fig. 2B).

### *Histomorphometrical differences in trabecular bones of PXRKO mice*

We next employed histomorphometrical analysis with tetracycline and calcein double labeling to evaluate bone turnover in WT and PXRKO animals. Gross observation of trabecular bone in the proximal tibia revealed decreased trabeculae and narrower interval between double labelings (Fig. 3A). Measurement of histomorphometrical parameters revealed that the BV/TV of WT mice was 23·18±1·54%. In contrast, the BV/TV of PXRKO mice was 9·32±1·47% ($P<0·001$), indicating a remarkable reduction in bone mass in PXRKO mice (Fig. 3B). The BFR/BS (mm$^3$/mm$^2$ per year) in WT mice was 0·465±0·018, whereas it was reduced by half in PXRKO mice, 0·224±0·034 ($P<0·001$). The ES/BS ratio (ES/BS) in WT mice was 38·97±1·19%, whereas it was 49·49±2·16% ($P<0·001$) in PXRKO mice. The N.Oc/BS ratio (N.Oc/BS) in WT mice was 4·30±0·36 (N/mm), whereas it was 6·33±0·47 ($P<0·01$) in PXRKO mice, indicating increased osteoclast number in PXRKO mice

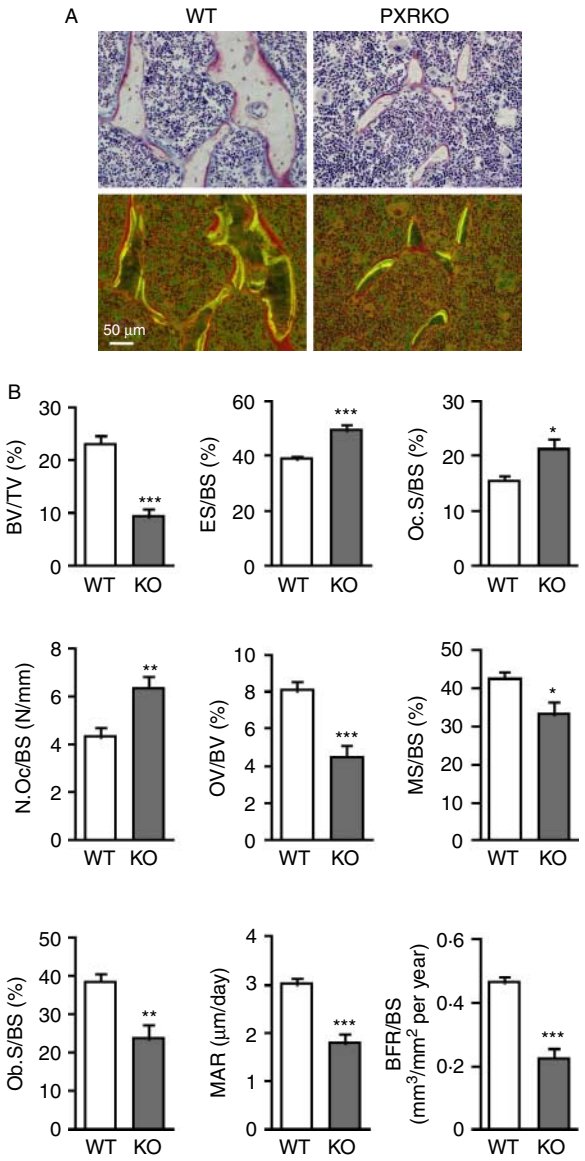


**Figure 3** Histomorphometrical differences in the trabecular bones of PXR knockout mice. (A) Representative cross-sectional images of the proximal tibial metaphyseal trabecular bones of wild-type (WT) and PXR knockout (PXRKO) mice. Microscopic views under incandescent light (upper panels) and fluorescent light (lower panels) are shown. Yellow and green lines of tetracycline and calcein labeling were visualized under fluorescent light. (B) Histomorphometrical parameters (BV/TV, bone volume fraction per tissue volume; ES/BS, eroded surface per bone surface; Oc.S/BS, osteoclast surface per bone surface; N.Oc/BS, number of osteoclasts per bone surface; OV/BV, osteoid volume fraction per bone volume fraction; MS/BS, mineralizing surface per bone surface; Ob.S/BS osteoblast surface per bone surface; MAR, mineral apposition rate; BFR/BS, bone formation rate per bone surface) of proximal tibial metaphyseal trabecular bones of wild-type (WT; $n=8$) and PXR knockout (KO; $n=8$) mice are shown. ***$P<0·001$; **$P<0·01$; *$P<0·05$. Full colour version of this figure available via http://dx.doi.org/10.1677/JOE-10-0208.

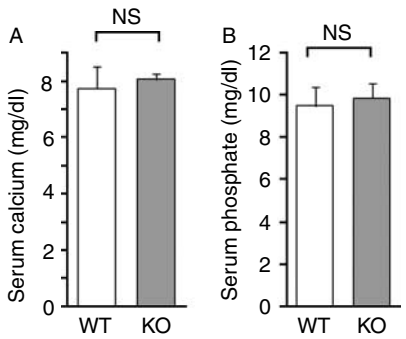


**Figure 4** Serum concentrations of calcium and inorganic phosphate. Values of calcium concentrations (A) and inorganic phosphate concentrations (B) are shown. No statistically significant difference was found between wild-type (WT; $n=4$) and PXR knockout (KO; $n=4$) mice.

(Fig. 3B). Taken together, these values indicate reduced bone formation and enhanced bone resorption in PXRKO mice.

Among the osteoclasts in WT mice, the N.Mo.Oc./BS ratio (N.Mo.Oc./BS) was $1{\cdot}63\pm0{\cdot}28$ (N/mm), whereas the N.Mu.Oc./BS ratio (N.Mu.Oc./BS) was $2{\cdot}66\pm0{\cdot}27$. On the other hand, N.Mo.Oc./BS in PXRKO mice was $2{\cdot}45\pm0{\cdot}37$, while N.Mu.Oc./BS was $3{\cdot}87\pm0{\cdot}34$. The ratio of N.Mo.Oc./N.Mu.Oc. was not significantly different between WT and PXRKO mice ($P=0{\cdot}82$).

Interestingly, OV index (OV/BV), which would have been increased in hypophosphatemia, was rather decreased in PXRKO mice (Fig. 3B). This suggests that PXRKO mice are not hypophosphatemic, which is in contrast with a recent report (Konno *et al.* 2010). We also demonstrate that PXRKO mice display no changes in serum calcium (Fig. 4A) and inorganic phosphate (Fig. 4B) concentrations, consistent with the hypothesis that SXRKO mice are not hypophosphatemic.

### *Histomorphometrical differences in cortical bones of PXRKO mice*

Having demonstrated a reduction in trabecular structure accompanied by enhanced resorption and reduced bone deposition, we next performed histomorphometrical examination of the femoral cortical bones from WT and PXRKO mice. Gross images of the femoral section revealed that the posteromedial endosteal surface of PXRKO mice was labeled with tetracycline and calcein, while an eroded anterolateral endosteal surface was observed in PXRKO mice (Fig. 5A). This indicates that, in contrast to WT mice, a posteromedial modeling process was underway in PXRKO mice. Measurement of histomorphometrical parameters revealed reduced cortical area and width (Fig. 5B).

To evaluate whether morphological phenotype of the femoral cortical bones in PXRKO mice actually caused mechanical fragility, three-point bending test was performed. In PXRKO mice, both of the two mechanical parameters calculated, stiffness and the maximum load, were decreased (Fig. 5C), indicating mechanical weakness in the femoral bones of PXRKO mice.

## Discussion

The data presented above provide important new information defining an important role for SXR/PXR in bone metabolism. The current results demonstrate that systemic SXR/PXR deficiency results in osteopenia with mechanical fragility, thus confirming the importance of this nuclear receptor as a regulator of bone homeostasis.

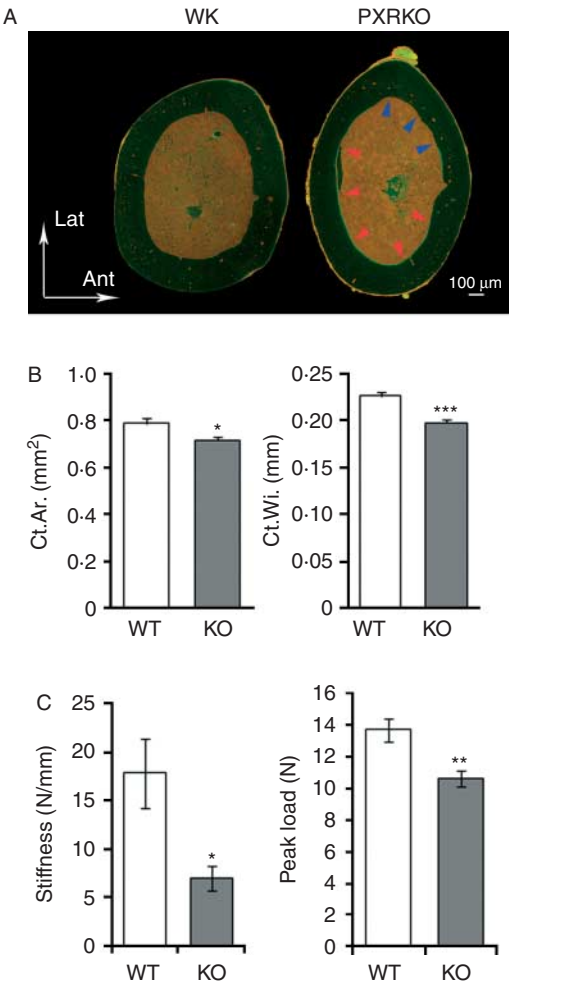


**Figure 5** Histomorphometrical differences in the cortical bones of PXR knockout mice. (A) Representative cross-sectional images of the femoral cortical bones of wild-type (WT) and PXR knockout (PXRKO) mice. Microscopic views under fluorescent light are shown. Upper direction in the figure corresponds to lateral direction, and right direction in the figure corresponds to anterior direction in the actual setting. Bone forming posteromedial endosteal surface labeled with tetracycline and calcein was indicated with red arrows. Bone resorbed anterolateral endosteal surface was indicated with blue arrows. (B) Cortical area (Ct.Ar.) and cortical width (Ct.Wi.) of the femoral cortical bones of wild-type (WT; $n=8$) and PXR knockout (KO; $n=8$) mice are shown. $^{***}P<0{\cdot}001$; $^{*}P<0{\cdot}05$. (C) Stiffness and the peak load were calculated by three-point bending test of femoral diaphysis of wild-type (WT; $n=8$) and PXR knockout (KO; $n=8$) mice are shown. $^{**}P<0{\cdot}01$; $^{*}P<0{\cdot}05$.

Concordant with reduced BMD, decreased trabeculae and cortical thickness were observed in PXRKO mice. The increased SMI score in PXRKO mice suggested the presence of a fragile, rod-like trabecular structure, which leads to mechanical fragility. The observation of continuing modeling process of the endosteal surface of femoral cortical bones also implied mechanical weakness of bones in PXRKO mice. In PXRKO mice, the modeling process was still observed at 4 months of age, indicating that a shift in BV to adjust for mechanical stress was still necessary. Histomorphometrical analysis of trabecular bones showed that bone formation parameters were decreased, while bone resorption parameters were increased in PXRKO compared with WT mice. We infer that SXR/PXR loss-of-function resulted in suppressed osteoblastic function and increased osteoclastic function, which is compatible with osteopenia. From the observed N.Mo.Oc. and N.Mu.Oc., the proportion of these two types of osteoclasts was almost the same in WT mice and PXRKO mice. Considering that multinuclear osteoclasts are functionally activated, the increased osteoclastic function in PXRKO mice can be explained by increased whole N.Oc rather than by activation of individual osteoclasts. This issue should be clarified by functional studies in the future.

We previously showed by *in vitro* analysis that vitamin K treatment induced the expression of several SXR/PXR-dependent genes (Ichikawa *et al.* 2006). One of the induced genes *CD14*, which affects osteoblastogenesis and osteoclastogenesis, could explain the *in vivo* effect of SXR/PXR function in this study. Igarashi *et al.* identified *Msx2* as a SXR/PXR target gene in osteoblasts. Notably, *Msx2* is a transcription factor promoting osteoblastogenesis, which could also explain the direct *in vivo* effect of SXR/PXR in bone tissue.

Since PXRKO mice lack the expression of PXR throughout the body, it is conceivable that the osteopenic phenotype could be due to SXR/PXR functions outside the bone tissue. Recently, Konno *et al.* reported an interesting indirect bone effect of SXR/PXR through induction of SLC34A2. They showed decreased BMD and hypophosphatemia in PXRKO mice and argued that the lack of SLC34A2 induction was responsible for these phenotypes (Konno *et al.* 2010). SLC34A2 is a phosphate transporter expressed in the intestine and kidney. Although their report is persuasive and intriguing, the reduced OV observed in our study indicated that other mechanisms may be at work because increased OV is a hallmark of osteopenia due to hypophosphatemia (Harrell *et al.* 1985). Moreover, our PXRKO animals did not exhibit elevated serum calcium or phosphate (Fig. 4A and B). SXR/PXR was also shown to affect calcium and phosphate homeostasis through the induction of vitamin D-catabolizing enzyme CYP3A4 in the liver and intestine (Zhou *et al.* 2006*a*). In this mechanism, activation of SXR/PXR in the liver and intestine would favor bone loss in WT mice. However, our work and that of other laboratories clearly indicates that SXR/PXR is required as a positive regulator of bone homeostasis. Thus, the overall conclusion we draw is that while activation of hepatic or intestinal SXR/PXR may have some unfavorable influences on bone metabolism, on balance, the presence and activation of SXR/PXR in bone is required to maintain proper bone homeostasis.

Another possible indirect action of SXR/PXR in bone involves its action as a suppressor of nuclear factor kappa-B (NF-κB) signaling. We and others previously reported SXR/PXR-dependent NF-κB inhibition (Gu *et al.* 2006, Zhou *et al.* 2006*b*). The expression of NF-κB target genes was elevated in all tissues tested in PXRKO mice (although bone was not examined). NF-κB signaling was reported to promote osteoclastogenesis (Jimi *et al.* 2004) and to inhibit bone formation by mature osteoblast (Chang *et al.* 2009). Therefore, increased NF-κB signaling and consequent enhancement of osteoclast function together with the suppression of osteoblastic function would be a reasonable explanation for the phenotypes observed.

In conclusion, the data presented above show that PXRKO mice are osteopenic. Micro-CT and histomorphometrical analyses were performed for the first time for PXRKO mice; fragile three-dimensional bone structure, suppressed bone formation, and enhanced bone resorption were observed. Further studies such as functional analysis of bone cells and selective ablation of PXR in bone cells will aid in understanding the precise role of SXR/PXR signaling in bone homeostasis, how this receptor exerts its osteoprotective effects, and could provide novel therapeutic targets for osteoporosis.

## Declaration of interest

The authors declare that there is no conflict of interest that could be perceived as prejudicing the impartiality of the research reported.

## Funding

This work was supported by grants from the Genome Network Project and DECODE from the Ministry of Education, Culture, Sports, Science and Technology, Grants from the Japan Society for the Promotion of Science, Grants-in-Aid from the Ministry of Health, Labor and Welfare (SI), a grant from the National Institute of Environmental Health Sciences (BB), and a predoctoral fellowship from the National Cancer Institute (SCC).

## Acknowledgements

We thank Dr Masami Muramatsu (Research Center for Genomic Medicine, Saitama Medical University) for critical discussion.

## References

Albermann N, Schmitz-Winnenthal FH, Z'graggen K, Volk C, Hoffmann MM, Haefeli WE & Weiss J 2005 Expression of the drug transporters MDR1/ABCB1, MRP1/ABCC1, MRP2/ABCC2, BCRP/ABCG2, and PXR in peripheral blood mononuclear cells and their relationship with the expression in intestine and liver. *Biochemical Pharmacology* **70** 949–958. (doi:10.1016/j.bcp.2005.06.018)

Azuma K, Urano T, Ouchi Y & Inoue S 2009 Vitamin K2 suppresses proliferation and motility of hepatocellular carcinoma cells by activating steroid and xenobiotic receptor. *Endocrine Journal* **56** 843–849. (doi:10.1507/endocrj.K09E-108)

Blumberg B, Sabbagh W Jr, Juguilon H, Bolado J Jr, van Meter CM, Ong ES & Evans RM 1998 SXR, a novel steroid and xenobiotic-sensing nuclear receptor. *Genes and Development* **12** 3195–3205. (doi:10.1101/gad.12.20.3195)

Chang J, Wang Z, Tang E, Fan Z, McCauley L, Franceschi R, Guan K, Krebsbach PH & Wang CY 2009 Inhibition of osteoblastic bone formation by nuclear factor-κB. *Nature Medicine* **15** 682–689. (doi:10.1038/nm.1954)

Cockayne S, Adamson J, Lanham-New S, Shearer MJ, Gilbody S & Torgerson DJ 2006 Vitamin K and the prevention of fractures: systematic review and meta-analysis of randomized controlled trials. *Archives of Internal Medicine* **166** 1256–1261. (doi:10.1001/archinte.166.12.1256)

Gu X, Ke S, Liu D, Sheng T, Thomas PE, Rabson AB, Gallo MA, Xie W & Tian Y 2006 Role of NF-κB in regulation of PXR-mediated gene expression: a mechanism for the suppression of cytochrome P-450 3A4 by proinflammatory agents. *Journal of Biological Chemistry* **281** 17882–17889. (doi:10.1074/jbc.M601302200)

Harrell RM, Lyles KW, Harrelson JM, Friedman NE & Drezner MK 1985 Healing of bone disease in X-linked hypophosphatemic rickets/osteomalacia. Induction and maintenance with phosphorus and calcitriol. *Journal of Clinical Investigation* **75** 1858–1868. (doi:10.1172/JCI111900)

Ichikawa T, Horie-Inoue K, Ikeda K, Blumberg B & Inoue S 2006 Steroid and xenobiotic receptor SXR mediates vitamin K2-activated transcription of extracellular matrix-related genes and collagen accumulation in osteoblastic cells. *Journal of Biological Chemistry* **281** 16927–16934. (doi:10.1074/jbc.M600896200)

Igarashi M, Yogiashi Y, Mihara M, Takada I, Kitagawa H & Kato S 2007 Vitamin K induces osteoblast differentiation through pregnane X receptor-mediated transcriptional control of the Msx2 gene. *Molecular and Cellular Biology* **27** 7947–7954. (doi:10.1128/MCB.00813-07)

Jimi E, Aoki K, Saito H, D'Acquisto F, May MJ, Nakamura I, Sudo T, Kojima T, Okamoto F, Fukushima H *et al.* 2004 Selective inhibition of NF-κB blocks osteoclastogenesis and prevents inflammatory bone destruction *in vivo*. *Nature Medicine* **10** 617–624. (doi:10.1038/nm1054)

Konno Y, Moore R, Kamiya N & Negishi M 2010 Nuclear xenobiotic receptor PXR-null mouse exhibits hypophosphatemia and represses the Na/Pi-cotransporter SLC34A2. *Pharmacogenetics and Genomics* **20** 9–17. (doi:10.1097/FPC.0b013e328333bb28)

Luo G, Ducy P, McKee MD, Pinero GJ, Loyer E, Behringer RR & Karsenty G 1997 Spontaneous calcification of arteries and cartilage in mice lacking matrix GLA protein. *Nature* **386** 78–81. (doi:10.1038/386078a0)

Miki Y, Suzuki T, Tazawa C, Blumberg B & Sasano H 2005 Steroid and xenobiotic receptor (SXR), cytochrome P450 3A4 and multidrug resistance gene 1 in human adult and fetal tissues. *Molecular and Cellular Endocrinology* **231** 75–85. (doi:10.1016/j.mce.2004.12.005)

Price PA, Otsuka AA, Poser JW, Kristaponis J & Raman N 1976 Characterization of a γ-carboxyglutamic acid-containing protein from bone. *PNAS* **73** 1447–1451. (doi:10.1073/pnas.73.5.1447)

Rüegsegger P, Koller B & Müller R 1996 A microtomographic system for the nondestructive evaluation of bone architecture. *Calcified Tissue International* **58** 24–29. (doi:10.1007/BF02509542)

Shiraki M, Shiraki Y, Aoki C & Miura M 2000 Vitamin K2 (menatetrenone) effectively prevents fractures and sustains lumbar bone mineral density in osteoporosis. *Journal of Bone and Mineral Research* **15** 515–521. (doi:10.1359/jbmr.2000.15.3.515)

Staudinger JL, Goodwin B, Jones SA, Hawkins-Brown D, MacKenzie KI, LaTour A, Liu Y, Klaassen CD, Brown KK, Reinhard J *et al.* 2001 The nuclear receptor PXR is a lithocholic acid sensor that protects against liver toxicity. *PNAS* **98** 3369–3374. (doi:10.1073/pnas.051551698)

Synold TW, Dussault I & Forman BM 2001 The orphan nuclear receptor SXR coordinately regulates drug metabolism and efflux. *Nature Medicine* **7** 584–590. (doi:10.1038/87912)

Tabb MM, Sun A, Zhou C, Grün F, Errandi J, Romero K, Pham H, Inoue S, Mallick S, Lin M *et al.* 2003 Vitamin K2 regulation of bone homeostasis is mediated by the steroid and xenobiotic receptor SXR. *Journal of Biological Chemistry* **278** 43919–43927. (doi:10.1074/jbc.M303136200)

Villanueva AR & Lundin KD 1989 A versatile new mineralized bone stain for simultaneous assessment of tetracycline and osteoid seams. *Stain Technology* **64** 129–138.

Xie W, Barwick JL, Downes M, Blumberg B, Simon CM, Nelson MC, Neuschwander-Tetri BA, Brunt EM, Guzelian PS & Evans RM 2000 Humanized xenobiotic response in mice expressing nuclear receptor SXR. *Nature* **406** 435–439. (doi:10.1038/35019116)

Zhou C, Assem M, Tay JC, Watkins PB, Blumberg B, Schuetz EG & Thummel KE 2006*a* Steroid and xenobiotic receptor and vitamin D receptor crosstalk mediates CYP24 expression and drug-induced osteomalacia. *Journal of Clinical Investigation* **116** 1703–1712. (doi:10.1172/JCI27793)

Zhou C, Tabb MM, Nelson EL, Grün F, Verma S, Sadatrafiei A, Lin M, Mallick S, Forman BM, Thummel KE *et al.* 2006*b* Mutual repression between steroid and xenobiotic receptor and NF-κB signaling pathways links xenobiotic metabolism and inflammation. *Journal of Clinical Investigation* **116** 2280–2289. (doi:10.1172/JCI26283)

Zhou C, Verma S & Blumberg B 2009 The steroid and xenobiotic receptor (SXR), beyond xenobiotic metabolism. *Nuclear Receptor Signaling* **7** e001. (doi:10.1621/nrs.07001)

Received in final form 4 September 2010
Accepted 27 September 2010
Made available online as an Accepted Preprint
27 September 2010